sciendo

Polish Journal of Chemical Technology, 26, 2, 42—47, 10.2478/pjct-2024-0017

Exosome-hydrogels loaded with metal-organic framework improve skin aging by inhibiting oxidative stress

Li-Jie Li*, Qing-Ling Han, Wen-Jie Feng, Zhan-Peng Wang, Hong-Hua Li

Plastic Surgery Department of Medical Beauty Center, The First Dongguan Affiliated Hospital of Guangdong Medical University, Dongguan, Guangdong, China

Corresponding author: e-mail: jie1110@126.com

Solvothermal reactions of $Ba(NO_3)_2$ with 1,3,5-benzenetricarboxylic acid gave rise to a new coordination polymer of $[Ba_6(BTC)_4(H_2O)_9]$}n (**1** H_3BTC = benzenetricarboxylic acid). The complex **1** was characterized soundly by Fourier transform infrared (FT-IR) spectroscopy, elemental analysis (EA), single-crystal X-ray diffraction (SCXRD), and thermogravimetric analysis (TGA). The framework of **1** has high thermal stability and shows intense luminescence at room temperature. Hyaluronic acid (HA) and carboxymethyl chitosan (CMCS) have good biocompatibility, based on the chemical synthesis method, the HA/CMCS hydrogel was prepared. With exosomes as drug models, we further synthesized novel exosome-loaded metal gel particles and evaluated their effects on oxidative stress in human dermal fibroblasts.

Keywords: Ba(II) compound, luminescence, hydrogels, exosome, skin aging.

INTRODUCTION

The exosome is an extracellular vesicle secreted by a cell. They are less than 150 nm, have a phospholipid bilayer similar to that of cells, and are distributed with transmembrane proteins, cytoplasmic proteins, and RNAs. the interior of exosomes contains a series of proteins (cytoplasmic, growth factors, etc.) and miRNAs that convey specific functional cues. exosomes have important applications in dermatology based on their high biocompatibility and bioactivity[1, 2]. As active substances and carriers, exosomes can play an important role in the fields of scar removal, skin barrier tissue repair, wound healing, whitening, and anti-hair loss.

Oxidative stress (OS) is a condition in which the body produces excessive amounts of highly reactive molecules, such as reactive oxygen radicals (ROS) and reactive nitrogen radicals (RNS), when the body needs to remove aging cells from the body or when it is subjected to a variety of deleterious stimuli. The degree of oxidation exceeds that of oxidative removal, and the oxidative and antioxidative systems become imbalanced, resulting in tissue damage[3]. Thus, the nature of oxidative stress is a negative effect produced by free radicals in the body. Free radicals produced by oxidative stress can directly or indirectly oxidize or damage DNA, proteins, and lipids. They can induce mutations in genes, protein denaturation, and lipid peroxidation, resulting in physiological and pathological responses in cells and tissues.

Recently, too many effects have been invested in designing and constructing metal-organic frameworks (MOFs) with charming topological architectures. As newly emerging hybrid materials, MOFs reveal great application prospects in heterocatalysis, luminescence, magnetism, non-liner optics, gas separation and storage, and other fields[4–7]. Most of the reported interesting carboxylate-based MOFs indicate that polycarboxylic acid ligands are the effective organic frameworks for producing the MOFs on account of the diversified coordination modes of carboxylate groups and strong coordination affinity to metal ions[8–11]. 1,3,5-benzenetricarboxylic acid (H_3BTC) features a C_3-symmetry and has three carboxylate groups that can deprotonated into three different forms of H_2BTC^{2-}, $HBTC^{2-}$ and BTC^{3-} under different basic conditions. The unique C_3-symmetry, various coordination modes, and different deprotonated forms make them widely used to construct functional MOFs[12, 13]. Until now, most of the BTC-based MOFs are constructed from rare earth metal ions or transition metal ions, seldom of which are constructed from the alkaline earth metal ions[14–16]. In comparison with the transition metal ions, Ba(II) ion, as an alkaline earth metal ion, reveals a higher affinity to O-donors along with a larger ion radius. Thus, the Ba(II) ions can be easily bridged by the polycarboxylate ligands into ordered crystalline MOFs under appropriate conditions[17, 18].

With the rapid development of biotechnology, hydrogels have an epoch-making significance in biomedical tissue engineering[19]. Hydrogels are three-dimensional network structures formed by crosslinking of hydrophilic polymers, which have the advantages of low toxicity and high permeability and have been widely used as drug carriers[20, 21]. Hydrogels can be divided into natural hydrogels and synthetic hydrogels. The biocompatibility of synthetic hydrogels is poor and there may be toxicity in the degradation process, which limits their further application[22]. Hydrogels prepared from natural materials, such as hyaluronic acid, chitosan, cellulose, sodium alginate, etc., have good biocompatibility and biodegradability and have little stimulation to patients during use[23]. Yang et al. prepared multifunctional chitosan hydrogel based on the sol-gel method, which has good biocompatibility, antibacterial activity, and self-healing ability, and has an obvious improvement effect on skin aging[24].

In this paper, the H_3BTC was chosen to finish the assembly with the Ba(II) ions under conditions of solvothermal, creating a new coordination polymer in success, namely, $[Ba_6(BTC)_4(H_2O)_9]\}_n$ (**1** H_3BTC is benzenetricarboxylic acid). The complex **1**'s generation, crystal architecture, luminescent performance, and thermal behavior will be reported in the following. Based on chemical synthesis, HA/CMCS hydrogels were prepared and their internal microstructure was measured by SEM. Using it as a drug carrier, we further designed and synthesized exosome-loaded metal gel particles and investigated their regulatory role in skin aging. Treatment of human dermal fibroblasts with increasing concentrations of exosome-loaded metal gel particles significantly

up-regulated cellular SOD levels and down-regulated MDA levels, thereby inhibiting oxidative stress.

EXPERIMENTAL

Materials and instrumentation

In this paper, the chemical reagents applied were provided by commercial sources and they can be utilized directly. To analyze the elements of carbon and nitrogen together with hydrogen, elemental Vario EL III was employed. PANalytical X'Pert Pro diffractometer was applied to conduct the characterization of PXRD utilizing 1.54056 Å Cu Kα radiation at 0.05° step size. With the temperature between 30 and 800 °C, by utilizing NETSCHZ STA-449C, TGA was implemented at 10 °C per min increasing rate with N_2 flow. The Edinburgh Analytical instrument FLS920 was employed to determine the compounds' luminescent performance. The microstructure of the samples was characterized by a field emission Scanning electron microscope (FE-SEMS4800, Hitachi).

Hyaluronic acid (HA) carboxymethyl chitosan (CMCS), 1-Ethyl-3-(3-dimethylaminopropyl)carbodiimide (EDC), N-Hydroxysuccinimide (NHS) were purchased from Sinopod Chemical Reagents Co., LTD.

Synthesis of compound $[Ba_6(BTC)_4(H_2O)_9]\}_n$ (1)

The mixture generated from 0.200 mmol $Ba(NO_3)_2$, 0.15 mmol H_3BTC, 0.5 mL DMF, and 4.0 mL H_2O was placed into the small glass vial (20.0 mL) and then it was heated for 36 hours under a temperature of 110 °C. After cooling the above mixture to RT at 2 °C/min rate, the colorless massive crystals of complex **1** were produced with 37 percent yielding based on H_3BTC. Elemental analysis calcd. for the $C_{36}H_{29}O_{33}Ba_6$: H, 1.60 and C, 23.82. Found: H, 1.63, and C, 23.78. IR(KBr pallet, cm^{-1}): 3421(m), 2930(m), 1543(s), 1502(s), 1428(s), 1105(m), 1028(s), 926(s), 806(m), 735(s), 706(s), 679(s), 608(w), 548(w), 515(s).

X-ray crystallography

With the Oxford Xcalibu E diffractometer controlled by computer, the compound's single crystal X-ray diffraction study could be implemented at RT by applying graphite-monochromatized Mo-Kα radiation (where λ is 0.71073 Å). The complex's architecture could be solved by applying direct approaches and subsequently refined using full-matrix least-squares strategies through the program of *SHELXL*-2014 based on F^2 [25]. The **1**'s crystallographic data are concluded in Table 1.

Preparation and characterization for exosome-loaded metal gel

First, 1 g HA powder and 3 g CMCS powder dissolved in deionized water were weighed to form 1 wt% HA solution and 3 wt% CMCS solution. The EDC/NHS solution was added drop by drop to the HA solution and stirred rapidly for 30 min. Then, the HA solution and CMCS solution were added to the mold according to the same volume and stirred quickly. After that, the solution was placed at 4 °C overnight. Finally, after the chemical cross-linking was completed, the gel was formed, and the HA/CMCS hydrogel was prepared after cleaning with deionized water. The Ba(II) coordination polymer was immersed in the exosome solution after ultrasonic dispersion and added to the CMCS solution to prepare the exosome-loaded metal gel.

The microscopic morphology of the sample was observed by scanning electron microscope. Before the test, the sample was freeze-dried and sprayed with gold.

Table 1. The complex **1**'s crystal data

Formula	$C_{36}H_{29}O_{33}Ba_6$
Fw	1813.57
Crystal system	monoclinic
Space group	*C*2/c
a (Å)	10.8675(6)
b (Å)	17.3976(10)
c (Å)	25.5718(15)
α(°)	90
β(°)	97.968(6)
γ(°)	90
Volume ($Å^3$)	4788.1(5)
Z	4
Density (calculated)	2.516
Abs. coeff. (mm^{-1})	4.963
Total reflections	11581
Unique reflections	5115
Goodness of fit on F^2	1.084
Final *R* indices [I>2sigma(I^2)]	R=0.0627, wR_2= 0.1664
R (all data)	R=0.0674, wR_2= 0.1705

Exosome preparation

Fresh cow's milk was centrifuged at 4000 rpm for 30 min at 4 °C. Subsequently, sucrose density gradient centrifugation was performed, and the resulting MK--Exo was aseptically filtered through a 0.22-μm filter and stored at –80 °C. MK-Exo was fixed with 2% (w/v) paraformaldehyde at room temperature. samples were subsequently examined by transmission electron microscopy (TEM) (Hitachi, Japan).

Determination of SOD and MDA levels in cells

Human dermal fibroblasts (HDF) were obtained from Procell (Wuhan, China) and cultured in Dulbecco's Modified Eagle Medium (DMEM, Gibco, USA) supplemented with 10% of fetal bovine serum (FBS, Gibco, USA). The cells were plated into 96-well plate and cultured for 24 h. Subsequently, cells were treated with increasing concentrations of exosome for 24 h. After washing three times with PBS, the SOD and MDA levels of HDF were determined by WST-8 and MDA kits (Beyotime, Shanghai, China) according to the manufacturer's instructions. The OD value at 450 nm was determined using a microplate reader (BioRad, USA).

RESULTS AND DISCUSSION

Crystal structure of complex 1

The architectural study of X-ray displayed that the complex **1** was crystallized in a monoclinic space group of *C*2/c, revealing a 3-dimensional skeleton with 2D -Ba-O-Ba- inorganic connectivity. Each of the fundamental unit of the complex **1** is composed of 3 Ba(II) ions, 2 BTC^{3-}, four and a half aqua ligands. As shown in Figure 1a, Ba1 and Bas ions display nine-coordinated monocapped square prismatic geometries, while Ba2 shows an eight-coordinated square prismatic geometry.

The coordination polyhedron of {Ba1O_9} is defined through six carboxylic acid O atoms belong to 4 individual ligands of BTC^{3-} and three terminal aqua ligands. The coordination polyhedron of {Ba3O_9} is defined via seven carboxylic acid O atoms offered by five distinct BTC^{3-}, a terminal ligand of aqua, as well as one μ_2-aqua ligand. The coordination sites of Ba2 ion are taken over via seven carboxylic acid O atoms originate from a terminal ligand of aqua and 6 distinct BTC^{3-}. The bond distances of Ba-O around Ba(II) centers range from 2.702(9) Å to 3.043(8) Å that are all comparable with those of reported Ba(II)-based compounds[18]. In this framework, the BTC^{3-} ligand shows two different coordination modes of μ_6-O, (η^2-O, O'), (η^2-O'', O'''), O''', (η^2-O'''', O''''), O''''' and μ_7-(η^2-O, O'), O', O'', O'', O''', O'''', (η^2-O'''', O'''''). Through careful checking the structure, it can be found that three edges was shared by each polyhedron {Ba1O_9} with two polyhedrons {Ba3O_9} and another polyhedron {Ba1O_9}, three edges was shared by each polyhedron {Ba2O_8} with two polyhedrons {Ba3O_9} together with another polyhedron {Ba2O_8}, and four edges was shared by each polyhedron {Ba3O_9} with two polyhedrons {Ba3O_9} and two polyhedrons {Ba2O_8}. As shown in Figure 1b, such edge-shared connections of these polyhedrons further lead to the 2-dimensional -Ba-O-Ba- layer extending along plane *ac*. Eventually, these neighboring 2-dimensional inorganic -Ba-O-Ba- layers are connected through the BTC^{3-} into a 3-dimensional structure (Fig. 1c).

Powder X-ray diffraction pattern (PXRD) and thermogravimetric analysis (TGA)

As displayed in the Figure 2a, there exists a great consistency in the pattern of PXRD between polycrystalline samples and simulated pattern acquired from the data of single crystal diffraction data, confirming the complex **1**'s high purity of polycrystalline samples.

As exhibited in the Figure 2b, the complex's TGA curve reveals two major weightlessness processes between 30 and 800 °C. 8.96% of the first weightlessness appeared between 105 and 153 °C, which is associated with the loss of coordinated H_2O molecules, and the second weightlessness appeared between 320 and 450 °C that was resulted from the organic ligand decomposition. After decomposition, the product of 50.83% corresponds to the formation of BaO (calcd: 50.73%).

Photoluminescent property of 1

The luminescent spectra in the solid state of free H_3BTC and **1** have been detected at RT (Fig. 3). It can be discovered that the free ligand of H_3BTC can emit the fluorescence, at 441 nm, there exists the maximum wavelength of emission (where λ_{ex} is 330 nm), which is associated with H_3BTC π^* to n or π orbital charge transitions[26], and at 456 nm, the complex **1** exhibits an emission band under 330 nm excitation. The complex **1**'s emission spectrum is similar to the emission spectrum of free H_3BTC and reveals 15 nm red-shift in comparison with the red-shift of free H_3btc. As a result, the **1**'s emission may be mainly come from the π^* to n or π charge transitions in the ligand[27].

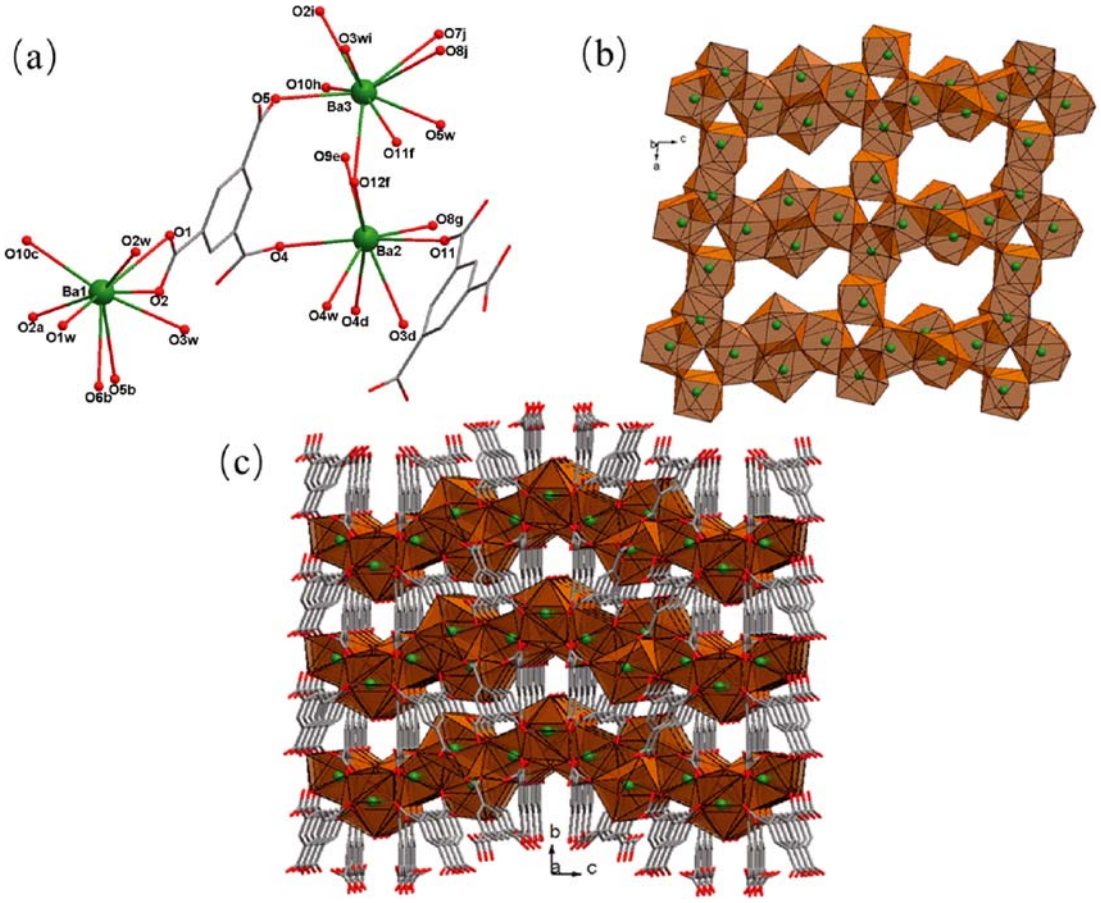

Figure 1. The coordination surroundings of the Ba(II) ion in complex **1** (a), The 2-dimensional -Ba-O-Ba- layer extending along plane ac (b), The compound's 3-dimensional structure viewing along the crystallographical axis *a* (c)

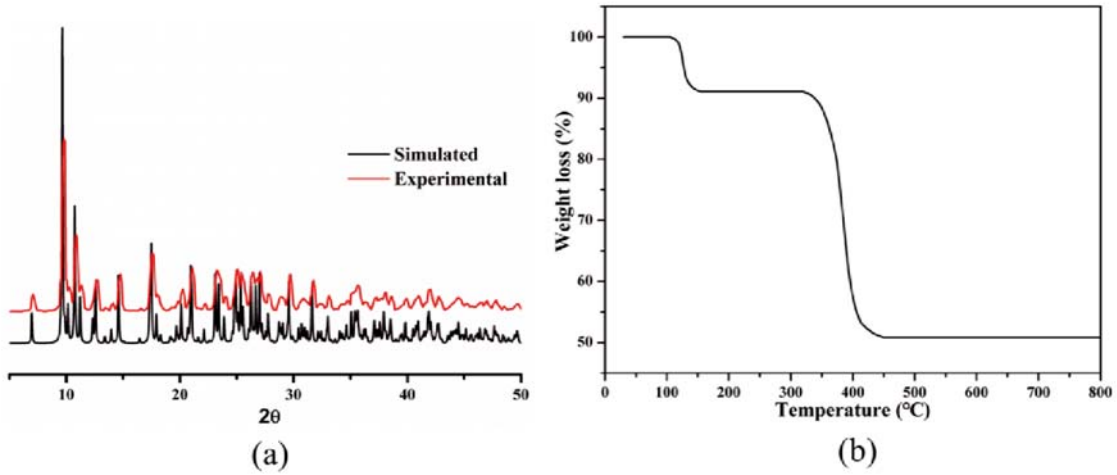

Figure 2. The complex's PXRD modes (a), and its TGA curve (b)

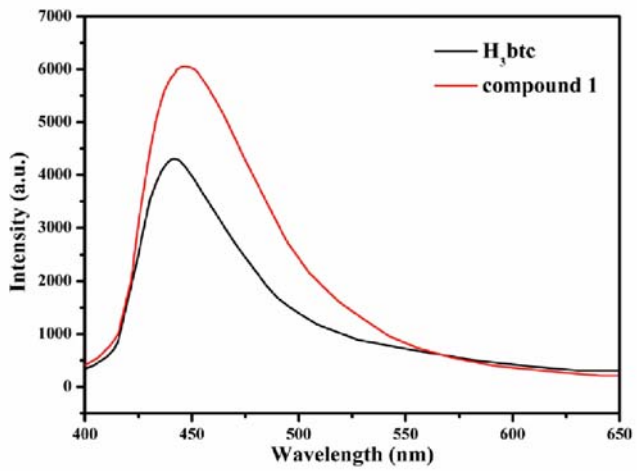

Figure 3. The luminescent emission spectra of free H_3BTC and the complex **1** at RT

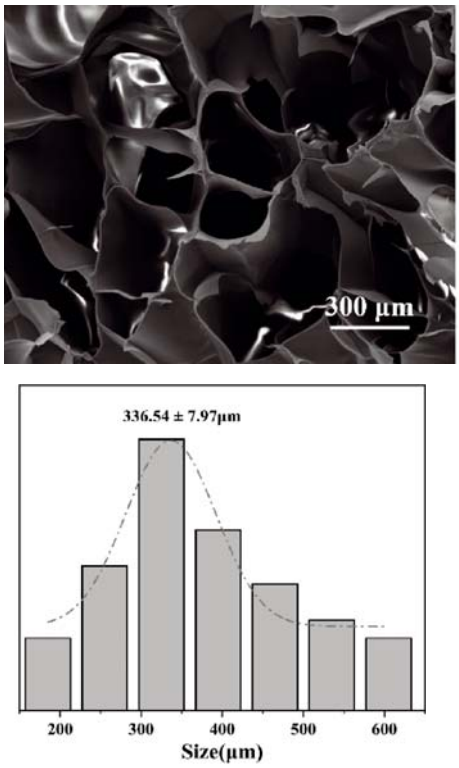

Figure 4. Microstructure and pore size distribution of HA/CMCS hydrogels

Micromorphology of the hydrogels

Hydrogel is a rapidly developing new functional polymer material, which is a three-dimensional spatial network structure composed of hydrophilic polymers. It has good biocompatibility and biodegradability, can effectively load and control the release of drugs embedded in hydrogels, and is an excellent drug carrier. We freeze-dried the prepared HA/CMCS hydrogel and observed the internal microstructure of the gel with scanning electron microscope. As shown in Figure 4, the freeze-dried gel showed a three-dimensional spatial network structure with interconnected holes. The pore size of the gel was concentrated at 336.54 ± 7.97 μm, and the gel had a large surface area, which could effectively load drugs.

Metallic gel particles loaded with exosomes significantly inhibit oxidative stress in skin cells

The morphological characteristics of exosomes were performed by TEM (Fig. 5). To verify whether exosome--loaded metal gel particles could improve skin aging, the levels of SOD and MDA, the main markers of oxidative stress, were detected after human dermal fibroblasts

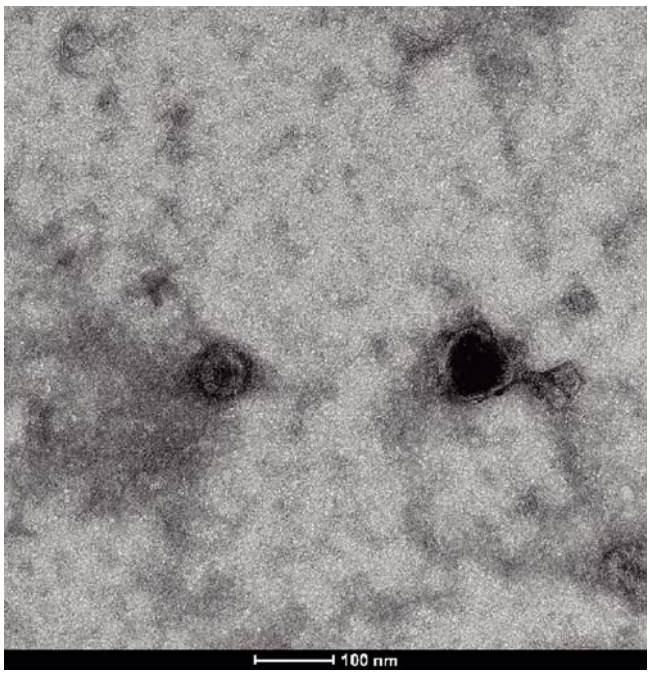

Figure 5. The characterization of exosomes by TEM

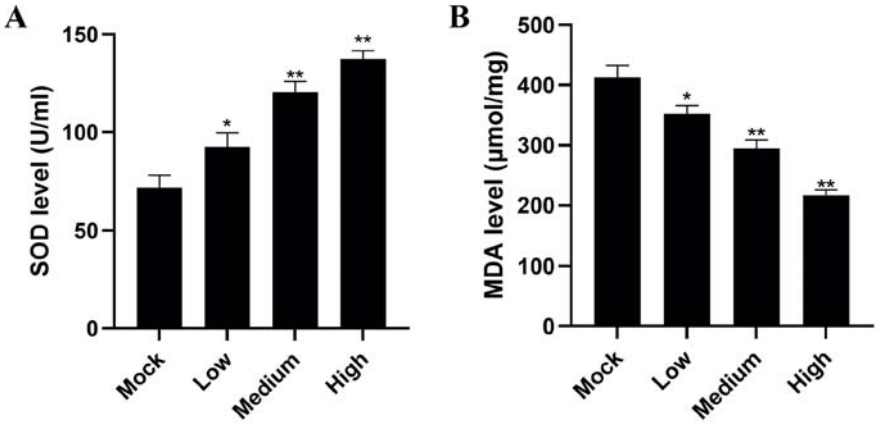

Figure 6. The effects of exosome-loaded metal gel particles on levels of SOD (A) and MDA (B) were measured. * indicated $P<0.05$, and ** indicated $P<0.01$

were treated with different concentrations of drugs for 24 hours. Cells treated with exosomes showed a significant increase in SOD levels and a significant decrease in MDA levels (Fig. 6), and the trend of these two metrics was drug concentration dependent. Our results suggest that exosome-loaded metal gel particles significantly inhibit the level of oxidative stress in skin cells.

CONCLUSION

In conclusion, we prepared a new Ba(II)-based compound *via* the self-assembly reaction of Ba(II) ions and 1,3,5-benzenetricarboxylic acid under solvothermal conditions. The BTC^{3-} ligands show two different kinds of coordination modes and connect all Ba(II) ions into a 3D framework having 2-dimensional -Ba-O-Ba- inorganic connectivity. The high thermal stability and intense luminescence emission of **1** indicated that it can be applied as an outstanding candidate for luminescent materials. HA and CMCS retain the biocompatibility of natural polysaccharides, and we successfully prepared HA/CMCS hydrogels based on chemical synthesis. The SEM results showed that the freeze-dried gel showed a three-dimensional porous structure, and the pores were connected with each other, and the pore size was concentrated in 336.54 ± 7.97 μm. Using exosomes as drug models, we further synthesized exosome-loaded metal gel and discussed their regulatory role in skin aging. Treatment of human dermal fibroblasts with different concentrations of exosome-loaded metal gel particles significantly up-regulated SOD levels and down-regulated MDA levels, thereby inhibiting oxidative stress. Our results suggest that exosome-loaded metal gel particles can be developed into a novel drug for improving skin aging.

ACKNOWLEDGMENTS

The research was supported by the level talent research funding program project of The First Dongguan Affiliated Hospital of Guangdong Medical University (GCC2023008).

LITERATURE CITED

1. Noonin, C. & Thongboonkerd, V. (2021). Exosome-inflammasome crosstalk and their roles in inflammatory responses. Theranostics, 11, 4436–4451. DOI: 10.7150/thno.54004.

2. Yang, B., Chen, Y. & Shi, J. (2019). Exosome Biochemistry and Advanced Nanotechnology for Next-Generation Theranostic Platforms. *Adv. Mater*. 31, e1802896. DOI: 10.1002/adma.201802896.

3. Kimball, J.S., Johnson, J.P. & Carlson, D.A. (2021). Oxidative Stress and Osteoporosis. *J. Bone Joint Surg. Am*. 103, 1451–1461. DOI: 10.2106/JBJS.20.00989.

4. Wu, Z.F. & Huang, X.Y. (2018). A mechanoresponsive fluorescent Mg-Zn bimetallic MOF with luminescent sensing properties. *ChemistrySelect*, 3, 4884–4888. DOI: 10.1002/slct.201800580.

5. Chen, Y.M., Zou, S.X., Tang, Y.M. & Hu, H.L. (2019). Two heterometallic coordination polymers based on Sr(II) ion and dicarboxylate ligand. Polyhedron, 159, 18–23. DOI: 10.1016/j.poly.2018.11.011.

6. Wu, Z.F., Gong, L.K. & Huang, X.Y. (2017). A Mg-CP with in situ encapsulated photochromic guest as sensitive fluorescence sensor for Fe^{3+}/Cr^{3+} Ions and nitro-explosives. *Inorg. Chem.* 56, 7397–7403. DOI: 10.1021/acs.inorgchem.7b00505.

7. Feng, Y.Q., Zhong, Z.G., Chen, S.Y., Liu, K.C. & Meng, Z.H. (2023). Improved Catalytic Performance toward Selective Oxidation of Benzyl Alcohols Originated from New Open-Framework Copper Molybdovanadate with a Unique V/Mo Ratio. *Chem. Eur. J*. 29, e202302051. DOI: 10.1002/chem.202302051.

8. Ji, W.J., Liu, G.F., Wang, B.Q., Lu, W.B. & Zhai, Q.G. (2020). Design of a heterometallic Zn/Ca-MOF decorated with alkoxy groups on the pore surface exhibiting high fluorescence sensing performance for Fe^{3+} and $Cr_2O_7^{2-}$. *Cryst. Eng.Comm*. 22, 4710–4715. DOI: 10.1039/D0CE00457J.

9. Lei, N., Wang, H., Fan, L. & Chen, X. (2024). Highly luminescent soft aggregates and films assembled by amphiphilic polyoxometalate complex in a polymerizable aprotic ionic liquid, *J. Photoch. Photobio. A*, 448, 115290. DOI: 10.1016/j.jphotochem.2023.115290.

10. Liu, L., Ran, Y., Gao, M., Zhao, X. & Mu, Y. (2021). Effect of solvent/auxiliary ligand on the structures of Cd(II) coordination polymers based on ligand 5-(2-benzothiazolyl) isophthalic acid. *Polyhedron*, 199, 115103. DOI: 10.1016/j.poly.2021.115103.

11. Lei, N., Li, W., Zhao, D., Li, W., Liu, X., Liu, L., Yin, J., Muddassir, M., Wen, R. & Fan, L. (2024). A Bifunctional Luminescence Sensor for Biomarkers Detection in Serum and Urine Based on Chemorobust Nickel(II) Metal-organic Framework, Spectrochim. *Acta A*, 306, 123585. DOI: 10.1016/j.saa.2023.123585.

12. He, J., Zhang, Y., Pan, Q., Yu, J., Ding, H. & Xu, R. (2006). Three metal-organic frameworks prepared from mixed solvents of DMF and Hac. *Micropor. Mesopor. Mater*. 90, 145–152. DOI: 10.1016/j.micromeso.2005.11.049.

13. Lian, T.T., Chen, S.M., Wang, F. & Zhang, J. (2013). Metal-organic framework architecture with polyhedron-in-polyhedron and further polyhedral assembly. *Cryst. Eng. Comm*. 15, 1036–1038. DOI: 10.1039/C2CE26611C.

14. Ozer, D., Oztas, N.A., Köse, D.A. & Sahin, O. (2018). Fabrication and characterization of magnesium and calcium trimesate complexes via ion-exchange and one-pot self-assembly reaction. *J. Mol. Struct*. 1156, 353–359. DOI: 10.1016/j.molstruc.2017.11.128.

15. Ma, K.R., Zhu, Y.L., Yin, Q.F., Hu, H.Y. & Ma, F. (2010). Structure and characterisation of a novel 3-D Ba(II)–MOF cased on the {Ba4O7} core. *J. Chem. Res.* 34, 705–709. DOI: 10.3184/030823410X12857507693391.

16. Li, W., Li, W., Liu, X., Zhao, D., Liu, L., Yin, J., Li, X., Zhang, G. & Fan, L. (2023). Two Chemorobust Cobalt(II) Organic Frameworks as High Sensitivity and Selectivity Sensors for Efficient Detection of 3-Nitrotyrosine Biomarker in Serum. *Cryst. Growth Des*. 23, 7716–7724. DOI: 10.1021/acs.cgd.3c00478.

17. Cao, K.L., Xia, Y., Wang, G.X. & Feng, Y.L. (2015). A robust luminescent Ba (II) metal–organic framework based on pyridine carboxylate ligand for sensing of small molecules. *Inorg. Chem. Commun*. 53, 42–45. DOI: 10.1016/j.inoche.2015.01.021.

18. Xin, X.H., Lu, W., Lu, J., Xu, J.G., Wang, S.H., Zheng, F.K. & Guo, G.C. (2018). A luminescent barium-based metal-organic framework: Synthesis, structure and efficient detection of 4-nitrobenzoic acid. *Inorg. Chem. Commun*. 97, 129–133. DOI: 10.1016/j.inoche.2018.09.029.

19. Chai, Q., Jiao, Y. & Yu, X. (2017). Hydrogels for biomedical applications: their characteristics and the mechanisms behind them. Gels, 3, 6. DOI: 10.3390/gels3010006.

20. Wei, L., Lin, J., Cai, C., Fang, Z. & Fu, W. (2011). Drug-carrier/hydrogel scaffold for controlled growth of cells. Eur. *J. Pharm. Biopharm*. 78, 346–354. DOI: 10.1016/j.ejpb.2011.01.015.

21. Chiani, E., Beaucamp, A., Hamzeh, Y., Azadfallah, M., Thanusha, A.V. & Collins, M.N. (2023). Synthesis and characterization of gelatin/lignin hydrogels as quick release drug carriers for ribavirin. *Int. J. Biol. Macromol*. 224, 1196–1205. DOI: 10.1016/j.ijbiomac.2022.10.205.

22. Larrañeta, E., Stewart, S., Ervine, M., Al-Kasasbeh, R. & Donnelly, R.F. (2018). Hydrogels for hydrophobic drug delivery. Classification, synthesis and applications. *J. Funct. Biomater*. 9, 13. DOI: 10.3390/jfb9010013.

23. Liao, J. & Huang, H. (2020). Review on magnetic natural polymer constructed hydrogels as vehicles for drug delivery. *Biomacromolecules*, 21, 2574–2594. DOI: 10.1021/acs.biomac.0c00566.

24. Yang, J., Chen, Y., Zhao, L., Feng, Z., Peng, K., Wei, A., Wang, Y., Tong, Z. & Cheng, B. (2020). Preparation of a chitosan/carboxymethyl chitosan/AgNPs polyelectrolyte composite physical hydrogel with self-healing ability, antibacterial properties, and good biosafety simultaneously, and its application as a wound dressing. *Compos. Part B: Eng*. 197, 108139. DOI: 10.1016/j.compositesb.2020.108139.

25. Sheldrick, G.M. (2015). Crystal structure refinement with SHELXL. *Acta Crystallogr., Sect. C: Struct. Chem*. 71, 3–8. DOI: 10.1107/S2053229614024218.

26. Zhang, X., Huang, Y.Y., Lin, Q.P., Zhang, J. & Yao, Y.G. (2013). Using alkaline-earth metal ions to tune structural variations of 1,3,5-benzenetricarboxylate coordination polymers. Dalton Trans., 42, 2294–2301. DOI: 10.1039/C2DT31536J.

27. Zhang, X., Huang, Y.Y., Zhang, M.J., Zhang, J. & Yao, Y.G. (2012). A series of Ca(II) or Ba(II) inorganic-organic hybrid frameworks based on aromatic polycarboxylate ligands with the inorganic M-O-M (M = Ca, Ba) connectivity from 1D to 3D. Cryst. Growth & Des., 12, 3231–3238. DOI: 10.1021/cg3003756.